ORIGINAL PAPER

A circular approach to foster additive manufacturing early design stages sustainability: a methodological proposal

Alberto Faveto[1,2] · Franco Lombardi[1] · Paolo Chiabert[1] · Frédéric Segonds[2]

Abstract

The design of new products is now influenced by shifting consumer demands and technological advancements. Products must satisfy high-quality standards and have a low environmental impact. New phenomena such as distributed and urban manufacturing are emerging to cope with this. A new manufacturing era is coming where methods that prevent waste, support small workshops and encourage do-it-yourself are crucial. In the early design stage, the process knowledge is minimal, and the decision taken is vital. For this reason, it is essential to support designers in anticipating the impact of decisions on the final product. This paper establishes the groundwork for decision-support methodologies for sustainable design in One-of-a-Kind additive manufacturing prototyping. Our proposed method is applied to a Fused Filament Fabrication case study, wherein we evaluate the impact of nine variables on factors such as process time, energy and material consumption, environmental footprint, and product quality. The initial step aims to generate fresh insights through Taguchi experimentation, while the subsequent step formulates and resolves a multi-objective optimization problem using the NSGA-II algorithm. The resulting Pareto-optimal solutions serve as the basis for a novel visual-based design support tool. The proposed approach can evaluate the trade-offs between product quality and environmental impact by offering users a visual heatmap based on quantitative data. This heatmap can guide the user in the material and production parameter selection. Integrating the decision support tool into the product design process can empower designers to create environmentally responsible products while fostering innovation.

Keywords Additive manufacturing · One-of-a-Kind production · Sustainability · Sustainable manufacturing · Multi-objective genetic algorithm · Design support tool

List of symbols

Acronyms

RMS	Reconfigurable manufacturing systems
UCD	User-centered design
AM	Additive manufacturing
OKP	One-of-a-Kind production
PLM	Product lifecycle management
MES	Manufacturing execution system
KBS	Knowledge-based system
ABS	Acrylonitrile butadiene styrene
PLA	Polylactic acid
FFF	Fused filament fabrication
DoE	Design of experiment
LiDs	Lifecycle design strategy
DIY	Do it yourself
CAD	Computer-aided design
CMM	Coordinate measuring machine
AMK	Additive manufacturing knowledge
EDK	Eco-design knowledge

✉ Alberto Faveto
  alberto.faveto@polito.it

1 Department of Management and Production Engineering, Politecnico di Torino, Corso Duca degli Abruzzi, 24, 10129 Turin, Italy

2 Laboratoire de Conception de Produits et Innovation LCPI, Arts et Métiers Institute of Technology, HESAM University, 151 Boulevard de l'hôpital, 75013 Paris, France

Variables and parameters

i	$i \in I(|I| = 32)$ Produced parts
k	$k \in K(|K| = 11)$ Primitive shapes (or subparts)
j	$j \in J \ (|J| = 7)$ Evaluators

|	
t	$t \in G$ Generations
PE_i	Energy Consumption
w_i	Material Consumption
PT_i	Processing Time
$totC_i$	Carbon Footprint
$\overline{A}_{ik}$	Accuracy Index
$\overline{R}_{ik}$	Resolution Index
$\overline{Q}_{ik}$	Qualitative Index
ke	CO_2eq emitted to produce a kWh of energy
EE	Embedded energy
C	CO_2eq emitted to produce a kg of material
q_{ikj}	Qualitative evaluation
MRE_{ik}	Maximum relative error
ARE_{ik}	Average relative error
T_{ik}	Number of points out of tolerance
D_{ik}	Range between the two farthest points
S_{ik}	Standard deviation of the point distances
M	Material
WT	Working temperature
PT	Plate temperature
WS	Working speed
S	Support
BAS	Base
LH	Layer height
IR	Infill rate
SN	Shell number
P_t	Initial population of the genetic algorithm
O_t	Offspring of the genetic algorithm
N	Population dimension of the genetic algorithm
X	Crossover factor of the genetic algorithm

1 Introduction

The development of the manufacturing industry is a dramatic sequence of changes in technologies and methodology that started at the beginning of the twentieth century with the production chain and mass production. The advent of numerical control machines in the 70 s triggered the period of flexible manufacturing, making it possible to produce several shapes with the same production line. In the 90 s, thanks to the theorization of reconfigurable manufacturing systems (RMS) [1], a new brick was added, producing different product shapes with a variable volume. Nowadays, the World is facing a new revolution in the manufacturing industry, characterized by the democratization of the product that entails several paradigms: Crowdsource Manufacturing [2], Cloud Manufacturing [3], Urban Manufacturing [4], and Social Manufacturing [5]. Although they differ in some aspects, it is possible to find some points in common. These paradigms are characterized by (i) an open or easy-to-share design approach, (ii) high personalization: each user/customer designs and produces his product, creating it himself from scratch, following some

design rules, or being supported by an expert designer or a crowd of them, and (iii) low production volume [6]. The shift toward a more democratized and inclusive approach to design and production in new manufacturing concepts is underscored by the pivotal role of User-Centered Design (UCD) [7]. UCD, places communities at the heart of the design process, ensuring that end-users have a meaningful and active role in shaping the products and systems that impact their lives. UCD is also crucial in selecting and implementing solutions that prioritize usability and bring value to all stakeholders [8]. By actively engaging with the target population, designers can gain valuable insights and feedback that inform the design decisions. This user-centered approach fosters a sense of ownership and empowerment among the community, as they become active participants in the design process enhancing both IP practices and creativity [9]. This work aims to create a design process that actively involves the user at every stage and raises their awareness about the environmental impact of their choices. This approach aligns with the principles of sustainable design and emphasizes the importance of considering the needs, preferences, and values of the user in order to develop solutions that are not only effective but also environmentally responsible [7].

According to the literature, it is clear that additive manufacturing (AM) is the most suited technology for high complexity, low volume, and high customization [10]. Moreover, the great majority of the platform that allows the sharing of design data and a democratized approach to manufacturing are based on AM, e.g., Makerbot Thingiverse, RepRap, GrabCAD, etc. [5].

In one-of-a-kind production (OKP), the probability of defective products is very high [8]; moreover, designers must test their ideas speedily and inexpensively. On the other side, a distributed approach to manufacturing can cause much waste and significantly impact the environment. In the OKP context, knowledge generation, storage, and reuse play a fundamental role. Bruno et al. [11] have proposed a paradigm that involves the integration of Product Lifecycle Management (PLM) system tools with the Manufacturing Execution Systems (MES), employing a central Knowledge Base System (KBS), allowing the communication between designers and the production line in both senses. This way, it is possible to manage design using data from production to minimize defects [12]. Figure 1 displays a graphical representation of the described paradigm.

For all these reasons, as highlighted by Bikas et al. [13], AM designers need to precognition the optimum process parameters and get insight from the production. Furthermore, a tool to make designers aware of quality's impact on cost and environmental impact is crucial [14]. The main research question this study want to address is to propose a simple and effective methodology that can provide adequate user insight into costs, environmental impacts, and
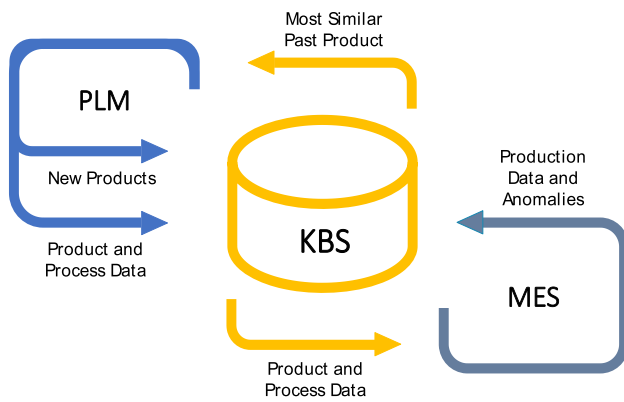
Fig. 1 Integration of PLM and MES through a central KBS, elaboration from Bruno et al. [11]

product quality for one-of-a-kind applications. In addition, the authors decided to emphasize the innovative aspect of circularity in AM, a topic still little explored by scholars. In particular, the topic of circularity in the presented approach sees the application of two fundamental concepts: (i) narrowing the loop of one-of-a-kind products by generating information in order to decrease waste in defects and testing, and (ii) closing the loop by assessing the impact of using a recycled material [15]. The study of the materials and their recyclability is another topic in recent scientific literature. Acrylonitrile butadiene styrene (ABS) and nylon are two of the most common materials used in FFF processes. These materials are derived from crude oil, and their recyclability is not widely spread [16]. For these reasons, the use of bio-based and biodegradable plastic in additive manufacturing is becoming increasingly important. PLA is a widely used plastic filament for FFF applications. Like the two precedent materials, PLA is not considered recyclable, although some studies on its recyclability are in progress. Nevertheless, it is bio-based since it is produced by corn starch and is biodegradable in industrial conditions. For this reason, its environmental impact is lower. In the literature, it is possible to find several examples of procedures and methodologies to recycle material for FFF applications [16, 17] and how the material behaves as a result of several recycling cycles [17]. By designing products with the intention of being recycled and incorporating recycled materials into the manufacturing process, waste generation can be minimized, and resources can be conserved. This not only reduces the environmental impact of the manufacturing process but also contributes to the efficient use of resources and the preservation of natural ecosystems.

Even if the proposed methodology could be used in batch production, our method is proper in distributed or small one-of-a-kind production contexts, which cannot rely on overly onerous tools. Moreover, defects and testing parts are not acceptable compared to batch production in those contexts. In particular, the authors decided to focus our analysis on Fused

Filament Fabrication (FFF) since, according to the literature, it is the most widely diffused AM technology for its cost-effective ratio [18]. This additive manufacturing technique is based on a continuous filament of thermoplastic material, heated, melted, and extruded through a nozzle. The nozzle deposits each layer, and the semi-liquid material hardens and adheres to the layers below. According to the literature, this technique is characterized by low cost and high manufacturing speed compared to other AM technology. However, the final results lack mechanical properties and surface quality [19]. Despite these limitations, it is the most promising additive manufacturing technology [18]. It is clear that the interest in studying a methodology to support the AM designer in decision-making in the early design stages [20]. Nevertheless, it is possible to perceived two main gaps: (i) the lack of a simple, standardized methodology to create and capitalize the knowledge in the additive manufacturing process to allow quicker and wasteless prototyping, and (ii) the lack of a method to generate knowledge related to the product cost and its environmental impact as well as the product quality, in order to foster its sustainability all along the lifecycle with a particular outlook on circularity.

The article is divided as follows: Sect. 2 details the proposed methodology. Section 3, describe a full case study of the proposed methodology. Finally, Sect. 4 presents some conclusions, impacts, and future developments of the study.

2 Methodology

A design optimization tool can be based on different approaches, in particular: (a) use the computer simulation to test design aspects' impact on final product performances, (b) use an analytical model based on physical law (white box modeling) to build a full optimization model, and (c) use an experimental data-driven approach (black box modeling) to estimate the relationships statistically [21]. Since the primary purpose of this work is to suggest an easy-to-replicate approach, the first two approaches (a–b) are not suitable candidates. Computer simulation needs previous knowledge and can be expensive in terms of costs and time. An analytical approach allows for achieving results in a fast and inexpensive manner. Nonetheless, an analytical approach needs a deep understanding of physical phenomena and complex mathematics to build deterministic functions. For these reasons, we decided to develop an experimental data-driven methodology to estimate the relationships between parameters and performances.

A possible idea for making an empirical approach work would be to integrate it with the knowledge of process experts. The model would optimize qualitative and quantitative performances, i.e., manufacturing cost and environmental impact (like manufacturing, use, etc.). Each of the decided
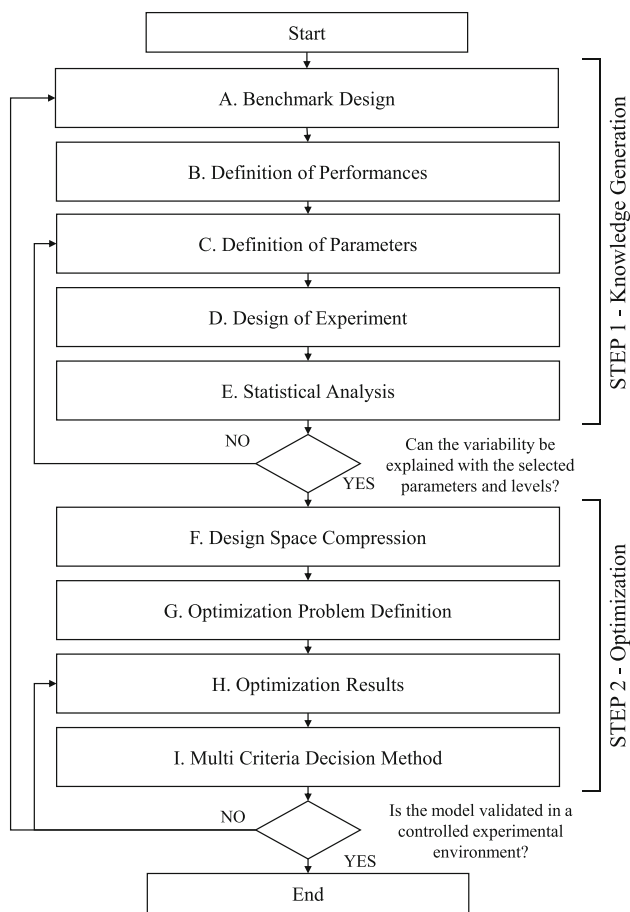
Fig. 2 Proposed Methodology divided into nine different stages

performances has to be weighted according to design decisions.

The proposed methodology is displayed in Fig. 2. It consists of two main phases: STEP 1—Knowledge Generation, whose goal is to define an experimental space assisted by experts to generate new knowledge, and STEP 2—Optimization, whose primary purpose is to capitalize on the acquired knowledge and define an automatized tool to support designers in choosing the best parameters and avoiding defects and wastes.

According to de Pastre et al. [22], creating a general standardized benchmark for experimentation is impossible. The design choice must be made by evaluating the experimental decisions and the metrological limits and specificity of the production process. Nevertheless, several guidelines exist, i.e., ISO 52902:2019 [23]. For all these reasons, the first step of our proposed methodology is to generate a new benchmark in order to satisfy three distinct aspects: (i) design choice, (ii) manufacturing constraints, and (iii) metrological limitations. After that, it is necessary to define some performances to be analyzed and the relative parameters. Then, according to all these variables, the authors defined a Design of Experiment (DoE) to investigate the impact of the selected parameters on

the performances. STEP 1 finishes with the statistical analysis of the obtained dataset in order to generate an empirical regression model to link the parameters mathematically with the performances. STEP 2 starts with the compression of the design space. If some parameter has no impact, they have to be removed. The same has to be done with performances that remain constant for all the experiments. Then, a multi-objective optimization problem is defined, and thanks to the obtained results, the designer can make his choice with precognition.

In the literature it is possible to find several decision support tools aiming to improve product sustainability by predict or monitor the manufacturing output and that provide valuable insights into optimizing energy consumption and surface product quality in traditional machining processes [24], these approaches can be applied to additive manufacturing as well. For instance, in [25] the authors propose a model based on artificial neural networks to predict the effects of cutting parameters on power, cutting force, surface quality, and material removal rate to reduce waste and improve energy efficiency and process sustainability. While in [26] the authors employ a multi-objective optimization method that aims to increase the quality of machined products while minimizing energy consumption.

In [27], the authors proposed a methodology to facilitate sustainable design thinking with an outlook on the product lifecycle. The proposed method is based on a Lifecycle Design Strategy (LiDS) wheel, two technical cards containing information on additive manufacturing processes and materials to support convergent thinking, and a SWOT (Strength, Weakness, Opportunity, Threat) framework to evaluate the obtained solutions. Laverne et al. developed a tool to support eco-additive manufacturing. In particular, their prototype is intended to guide the designer through a user interface in the machine choice that satisfies the product specifications and the machine parameters able to drive the decided resource minimization strategy [28]. Rocheton et al. proposed a similar tool to assist designers in making conscious environmental choices. The tool inputs the user skills, the mesh file, the design rules, and the strategy the user wants to follow (minimize energy or material consumption), and it gives the ideal machine to produce the prototype, the printing orientation, and parameters [29].

Agrawal proposes an approach, suggesting a combination of Design for Additive Manufacturing and Design for Environment rules. In particular, he found 26 design guidelines clustered into four groups, i.e., (i) accuracy, (ii) layer thickness, (iii) Strength, and (iv) environmental and end of life, and he ranked the 26 guidelines with a TOPSIS-based multi-criteria decision method to facilitate the designers in their choice [30]. The proposed approach differs from those found in the literature since it is a quantitative approach consisting

of a knowledge generation phase and a multiobjective optimization phase. These two features are particularly suitable for OKP productions since there is no in-depth knowledge of the possible output results and it is very important to try to optimize various trade-offs (e.g., quality cost and sustainability) A similar approach is already used in the literature. For instance, in [31], the authors apply an empirical methodology to evaluate and estimate the optimum drilling rate and electrode wear ratio in electric discharge machining drilling, while in [32], a comparable method is used to identify the best parameters to maximize product performances (warpage, weld line, and clamp force) in plastic injection molding processes. However, the integration of this type of procedure in additive manufacturing has not yet found much space in the scientific literature. The authors applied the proposed approach to a real case study in the following two sections of this article.

3 Case study

3.1 Experiment setup

The experimentation is performed in the Arts et Metiers Institute of Technology's Laboratoire Conception de Produits et Innovation (LCPI) using a Raise 3D E2, a desktop additive manufacturing machine for FFF application with two independent extruders. This tool is economical and adapted to do-it-yourself (DIY) or FabLab applications. The benchmark is designed with FreeCad (v0.19), an open-source parametric 3D Computer-Aided Design (CAD) modeler. Finally, the G-code generation is performed using the Raise 3D E2's proprietary slicer IdeaMaker (v4.2.3). The material used for this experiment is black PLA with a 1.75 mm diameter and a density equal to 1.24 g/cm^3, bought from the French company DailyFil.

3.2 Benchmark design

The design choice matches the experimental goals, production, and metrological limits, using ISO 52902:2019 as a reference [23]. The benchmark is defined in collaboration with additive manufacturing experts, knowing the machine's capabilities. On the other side, the authors decided on the dimension and position of different features to be capable of measuring them straightforwardly. The benchmark is adapted for prototyping assessment, and it contains the most frequent elementary shapes. Figure 3 displays the benchmark orthogonal projection of left, right, frontal, and top views emphasizing the key quotas.

The benchmark comprises eleven subparts: Bridge, Arc, Sphere, Holes, Pins, Side, Ribs, Slots, and three different Slopes (30°, 45°, and 60°). The subparts are intended to

Table 1 Benchmark subparts' goal definitions

Subparts	Goals
Bridge	Accuracy and surface texture
Arc	Accuracy and surface texture
Sphere	Accuracy and surface texture
Holes	Accuracy and surface texture
Pins	Accuracy, resolution, and surface texture
Side	Accuracy, resolution, and surface texture
Ribs	Accuracy, resolution, and surface texture
Slots	Accuracy and surface texture
60°, 45° and 30° Slopes	Accuracy and surface texture

assess various geometrical shapes' accuracy, resolution, and surface texture. Accuracy is the capability of the machine to build an object as close as possible to the reference value. The resolution is the potential to manufacture small dimension features, and finally, the surface texture is the capability to create a smooth surface without irregularities and nasty overhangs. In Fig. 4 the eleven subparts are defined and highlighted using different colors. Table 1 specifies the purpose of each subpart.

3.3 Definition of performances

It is possible to split the performances into two separate classes: (i) environmental-related performances and (ii) quality-related performances. The first group focused on energy consumption during manufacturing, material consumption needed to produce the part, and time necessary to make the part. At the same time, the quality of the object is evaluated through three different metrics. Each metric is intended to evaluate one specific goal for any subpart and uses various means. To assess the surface texture, the authors decided to analyze the part through a subjective assessment made by a sample of experts in diverse fields of product design. To evaluate the resolution of subparts, an analysis of the different dimensions is performed through a manual caliper and compute a global metric. Finally, a scanner is used to generate a product's cloud of points to compare the adherence between the produced part and the CAD. This final process is made to estimate a metric of the accuracy of the process. In the next sub-paragraphs, it is detailed how all (i) related environmental performances and (ii) quality-related performances are computed.

The authors decided to keep the economic aspect outside our analysis since all the presented performances can be cost-related. The direct impact of some of them, like energy or material consumption, can be effortlessly calculated. On
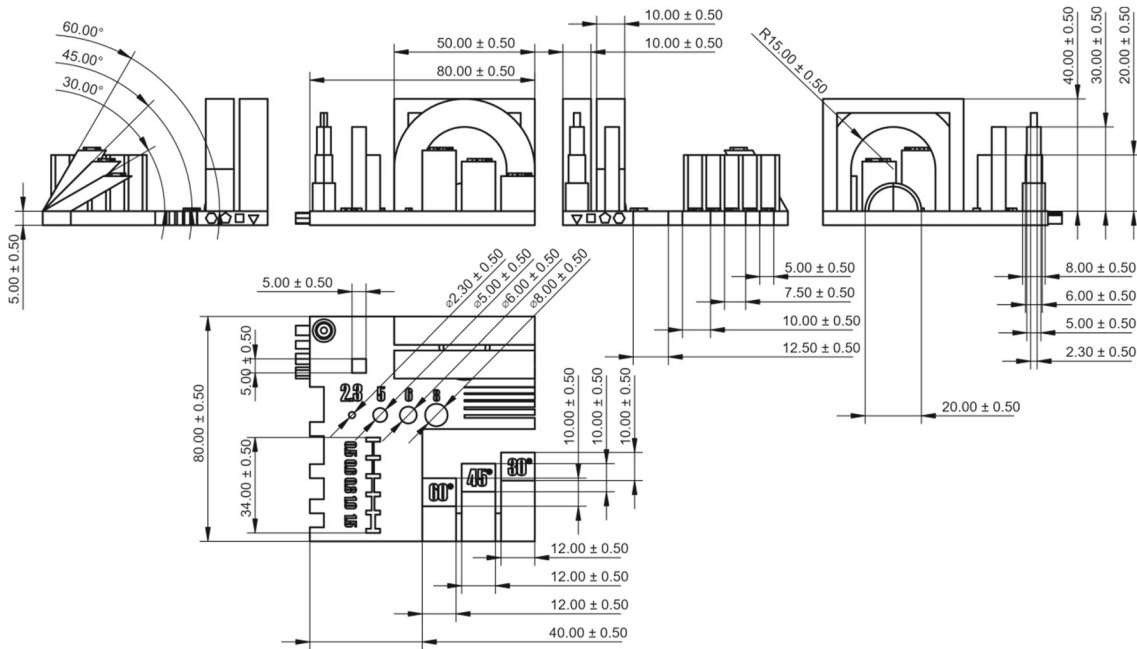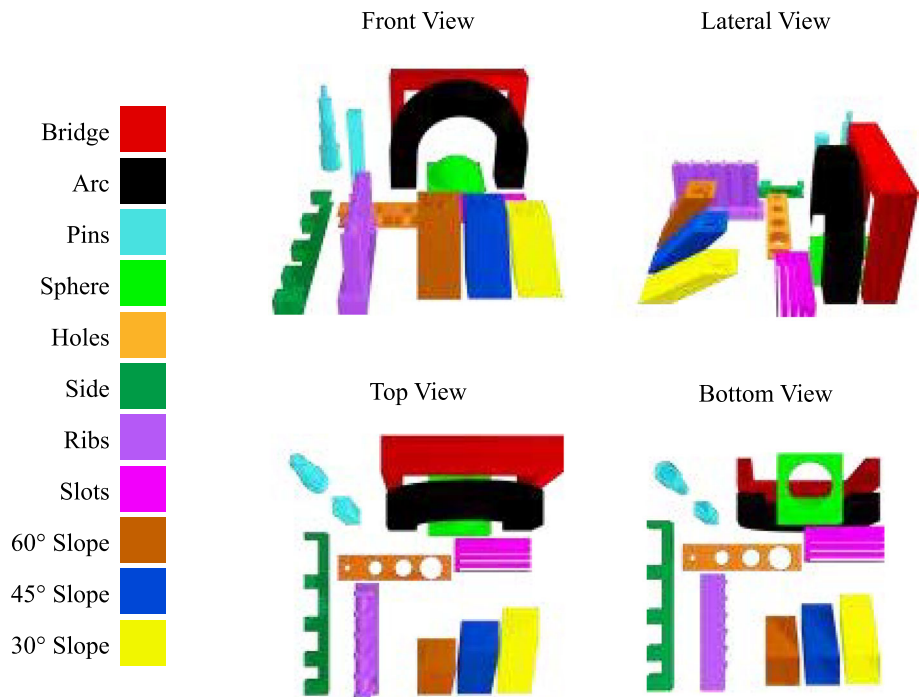
Fig. 3 Benchmark orthogonal projection (left, frontal, right, and top view) and 3D representation with the main dimensions

Fig. 4 Benchmark's subparts' graphical representation

the other hand, the economic impact of quality is hard to define. Moreover, each cost depends on the company ecosystem, suppliers, and stakeholders. Therefore, it is preferable to leave out the pure cost so that our analysis retains its value while changing the conditions of time and space. However, this study also has indirect economic aspects: higher material and energy consumption will result in higher costs for the company and a more significant environmental impact.

Table 2 summarises the seven performance indexes used for our experimentation and the measurement unit, classified into two groups: (i) environmental-related performances and (ii) quality-related performances. The following subparagraph illustrates each index's primary purpose and computation procedure.

Table 2 Performance definition

Class	Performance	Unit
Environmental-related performance	Energy consumption (PE_i)	VAh
	Material consumption (w_i)	g
	Processing time (PT_i)	s
	Carbon footprint ($totC_i$)	kg CO_2eq
Quality-related performance	Accuracy index ($\overline{A}_{ik}$)	%
	Resolution index ($\overline{R}_{ik}$)	%
	Qualitative index ($\overline{Q}_{ik}$)	%

3.3.1 Energy consumption

In order to measure the energy consumption, we installed an amperemeter in series and a voltmeter in parallel on the machine alimentation circuit. The sensors are the AC5712 current sensor and the ZMPT101B voltage sensor. Using an Arduino board, we measured the VRMS and ARMS each second to compute the apparent power in VA. After that, we used this value to calculate the whole energy consumption in VAh. VAh represents the apparent energy absorbed by the machine, and this value takes into account the active energy used by the device and the reactive power losses. Reactive power generates extra load, and the network must be appropriately sized. Furthermore, in industrial applications, reactive energy consumption can directly impact energy costs; from an environmental perspective, a VAh-based bill is preferable. Analyzing the phase shift between system voltage and current, when the machine is stopped, the cos φ is around 0.89, while when the device is running, it drops as low as 0.4 (where φ is the phase angle between the voltage and the current and cos φ represents the ratio between the real power and the apparent power). This significant variation is justified by the use of induction motors inside the machine that draw reactive power to operate. According to the literature, the energy consumption in AM can be computed per piece, weight, or volume of extruded material [21]. We decided to use the energy per piece since the produced part is a benchmark and has the same geometrical characteristics every time. Moreover, in FFF applications, it is more common to use this indicator.

3.3.2 Material consumption and processing time

We measured the total processing time needed to produce any part. After the production, we weight each piece to consider the total amount of PLA used. We compute the total amount of material used for the model and supports. The scale used for the analysis is a PCB 1000-2 by KERN &

SOHN GmbH. The scale resolution is equal to 0.01 g. The slicer also estimates these two values. Nevertheless, an average error on these valuations of 1337 s (4.06%) and 1.68 g (3.6%) is detected.

3.3.3 Carbon footprint

In order to evaluate the environmental impact of each product, we decided to estimate the production carbon footprint assessed in kg of CO_2eq. However, it is hard to consider a complete LCA in the first stages of product development since the information is missing. In contrast, the data is extensive in the advanced stages, but the possibility of significant product changes is minimal [33]. We proposed a semi-quantitative approach by estimating the kg of CO_2eq to give some insights to designers even if the knowledge of the process is still low. We decided to analyze the impact of the production in the first two steps of the product lifecycle: raw material extraction and manufacturing. In our experiment, the environmental impact of the i-th part is mainly composed of four elements: (i) the embodied energy committed to creating the needed quantity of plastic material. (ii) The kg of CO_2eq emitted in the atmosphere to produce that amount of plastic, and (iii) the direct energy consumed by the AM machine to produce the part. We decided not to evaluate the impact of the supply chain since we use a single supplier for raw material, and so the kg of CO_2eq emitted in the atmosphere for transportation, in our experiment, is a constant. Usually, the energy consumption in LCA analysis is not directly translated into kg of CO_2eq since the carbon footprint of electricity depends on the energy source used to make it. For instance, in the United States, energy is mainly produced from coal, oil, and gas. A considerable share of Germany's electric energy is produced from solar and wind plants, while France is 78% nuclear [34]. Nevertheless, our analysis made some assumptions about the energy production mix. We used the average French ones since the experiment was performed in France, and the material used was produced in the same country. France's energy mix is composed of 10% fossil fuel, 78% nuclear, and 12% renewable. The emission of such a combination is equal to 0.06 CO_2eq kg/kWh [35]. According to the literature, polylactic acid has an embedded energy of 15.28 kWh/kg (55 MJ/kg), producing 2.8 CO_2eq kg/kg. In comparison, the recycled counterpart has embedded energy equal to 5 kWh/kg (18 MJ/kg) and produces 0.95 CO_2eq kg/kg [35]. All the used values must be used with extreme caution, and for this reason, we defined our analysis as semi-quantitative. According to Ashby [35], a standard deviation of 10% on all average CO_2eq values must be considered. Finally, the amount of kg of CO_2eq emitted for any i-th parts ($totC_i$) is equal to:

$$totC_i = keEEw_i + Cw_i + kePE_i \qquad (1)$$

where ke is the amount of CO_2eq emitted to produce a kWh of energy (0.06 CO_2eq kg/kWh), EE is the embedded energy of the used material (e.g., for not recycled PLA 15.28 kWh/kg), w_i is the total amount of material used to produce the part (model + supports), C is the quantity of CO_2eq emitted to produce a kg of material (e.g., for not recycled PLA 2.8 CO_2eq kg/kg), and finally, PE_i is the total energy consumed by the machine to produce the i-th part.

3.3.4 Qualitative index

The first quality analysis is a quantitative one. We composed a panel of 8 design experts. Their domain is various: computer-aided design (CAD), industrial engineering, and AR and VR design, and we ask them to evaluate each part qualitatively. Some tools have been provided to facilitate their task: plates of the exact size of the slots and four different gauges with the precise diameter of the four holes. Moreover, we ask them to consider with particular notice the surface texture and the roughness of each part. We give them an evaluation sheet and ask them to assess each sub-part using a Likert scale between 1 and 7, 1 for the highest quality and 7 for the worst. After that, we composed an Index for each of the 11 subparts by averaging the nine evaluations. E.g., the quantitative index Q_{ik} of the k-th sub-parts present on the i-th part is calculated as:

$$Q_{ik} = \frac{\sum_{j=1}^{N} q_{ikj}}{J} \tag{2}$$

where q_{ikj} is the evaluation given by c on the k-th subpart present on the i-th produced piece, and J is the number of evaluators. In order to compare each indicator, we normalize them by dividing each value by the maximum value found using the formula:

$$\overline{Q}_{ik} = \frac{Q_{ik}}{\max(Q_{ik})} \tag{3}$$

According to Yu et al. [36], the proposed method is the best to normalize positive values since it can maintain the minimum and the maximum value and the relative difference between series elements. Thus, we ranged all indices between 0 and 1, where 0 indicates the best quality while 1 is the worst. In this way, both Environmental-Related Performances and Quality-Related Performances are concordant: the best performance is achieved with the minimum value.

3.3.5 Resolution index

The second quality analysis is related to achievable resolution. We performed this analysis only for 3 of the 11 sub-parts: Pins, Side, and Ribs. These three elements are designed to assess the minimum resolution of the machine

in manufacturing specific features. In particular, the first Pin is designed to determine the resolution of producing vertical cylinders with a diameter of 8, 6, 5 and 2.3 mm. The second Pin has a square base 5 mm wide and 35 mm in height. The Side can assess the manufacturing of an interlock 5, 7.5, 10, and 12.5 mm. Finally, the Ribs are intended to evaluate the production of a straight rib of 5 mm between two supports with a thickness of 1.5, 1, 0.8, 0.6, and 0.5 mm. In order to evaluate the resolution index, we measure all the presented dimensions with a manual caliper with 0.01 mm precision. For the three aforementioned k-th subparts present on the i-th produced piece, we calculate two different metrics: the average relative error ARE_{ik}, and the maximum relative error MRE_{ik}.

The resolution Index for the k-th sub-part on the i-th piece is the average of the metrics normalized using the previously presented method:

$$\overline{R}_{ik} = \frac{\overline{ARE}_{ik} + \overline{MRE}_{ik}}{2} \tag{4}$$

3.3.6 Accuracy index

The experimentation is composed of different steps: (i) CAD modeling, (ii) 3D model generation, (iii) Slicing, (iv) Production Process, (v) Scanning, and (vi) Sampling. Figure 5 displays the six tasks and the associated outputs (digital or physical). Moreover, the image shows where Accuracy Index ($\overline{A}_{ik}$) and the Resolution Index ($\overline{R}_{ik}$) are measured. The $\overline{R}_{ik}$ is calculated between the produced part and CAD quotas. In contrast, $\overline{A}_{ik}$ is evaluated between the mesh file (.stl), considered as a reference, and the final cloud of points (.asc). In this paragraph, we detail the different steps we followed in computing this index. Each intermediate step can generate variability, so it would be impossible to know where the measured error is generated.

To evaluate the accuracy of the part, we propose an automated methodology by scanning the produced part and comparing it with the mesh reference in stl format, in addition to the qualitative and quantitative methods presented above. According to the literature, there are no industrial applications of scanning procedures to evaluate product quality, and the most used methods are traditional calipers or coordinate measuring machines (CMM) [37]. However, it is possible to find some applications in scientific research. E.g., in [12], the authors proposed integrating a quality scan control system at the shop-floor level with the Manufacturing Execution System, while [38] proposed an online quality monitoring methodology to detect defects in material extrusion AM processes. We decided to use an optical scanner, the Einscan-SP, a 3D desktop scanner with a declared accuracy of 0.05 mm.

Fig. 5 Experiment Process Steps

A. flat   B. upside down   C. on flat side   D. on arc   E. on uneven side
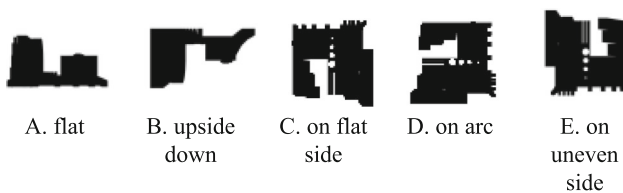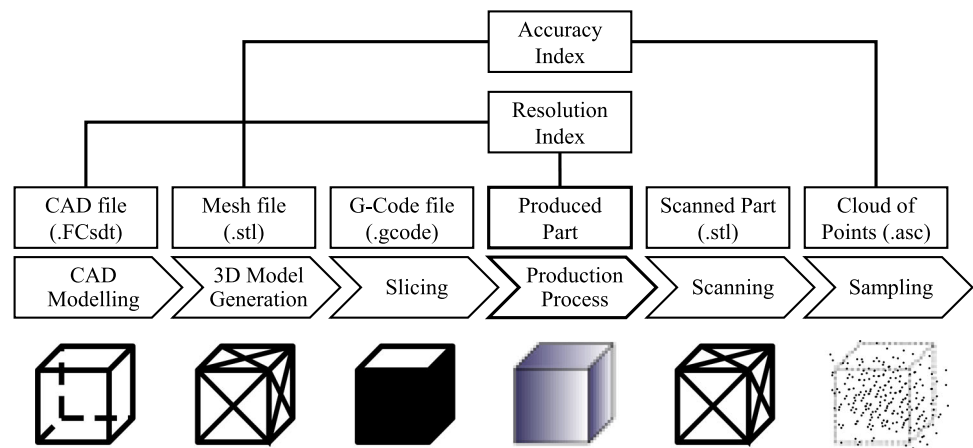
Fig. 6 The five different scanning positions used

The produced parts were scanned using an established procedure: each piece was covered by a layer of mattifying white spray to allow a clean and more detailed image. Then the part was scanned five times in different positions to analyze each side properly (see Fig. 6). The part was positioned on a turning table, and the scanner took a picture each 10°. Finally, the five different files were merged to create a single stl file.

In a second moment, we used the open-source software CloudCompare to generate a produced part cloud of points, each of which has approximately 10 M points. The cloud of points was then aligned to the reference mesh. Finally, we computed the signed distance between each point and the reference mesh. We can consider the mesh as a reference since the average error between the mesh surface, and the CAD surface is 0.011 μm with a standard deviation of 18.63 μm.

Using these distances between the scanned part and the reference mesh, we computed three metrics: the number of points outside the tolerance T_{ik}, the range between the two farthest points D_{ik}, and the standard deviation S_{ik}. According to the literature, in FFF applications, a satisfying accuracy is $\pm$ 0.5%, with a lower limit of $\pm$ 0.5 mm [39]. For these reasons T_{ik} was computed as the percentage of points outside the interval $\pm$ 0.5 mm. We also calculated the distance distribution's average, skewness, and kurtosis. These three other values could be used in further analysis. Finally, we computed the accuracy index $\overline{A}_{ik}$ for the k-th subpart present on the i-th piece, by averaging the three metrics normalized

Table 3 Design of experiment levels

Factors	Level (−)	Level (+)
Material (M)	Recycled PLA	Not Recycled PLA
Working temperature (WT)	200°	215 °C
Plate temperature (PT)	T_a	50 °C
Working speed (WS)	40 mm/s	80 mm/s
Support (S)	No	Yes
Base (BAS)	No	Yes
Layer height (LH)	0.1 mm	0.3 mm
Infill rate (IR)	10%	60%
Shell number (SN)	1	3

using the same methodology presented previously.

$$\overline{A}_{ik} = \frac{\overline{T}_{ik} + \overline{D}_{ik} + \overline{S}_{ik}}{3} \tag{5}$$

3.4 Definition of parameters

We have considered some parameters related to Product Material, Manufacturing Parameters, and Product Finesse. According to Laverne et al. [28], users who have scarce Additive Manufacturing Knowledge (AMK) and Eco-Design Knowledge (EDK) prefer to have simple guided parameters so they can spend the most time on creative design. For this reason, we decided to focus only on easily accessible parameters. We decided to analyze the impact of using a Recycled PLA instead of a normal one. Then we decided to investigate the parameter present on the first page of the Slicer Software used to create the Gcode (presence of support, presence of base, layer height, infill rate, shell number) and all the parameters suggested by the filament producer (working temperature, plate temperature, and working speed). Table 3 displays the experiment parameters levels (Factors). The

parameters WT, PT, and WS levels have been decided using the material manufacturer's suggested ranges as a reference. In contrast, the parameters LH, IR, and SN have been chosen by defining a wide range to explore as much design space as possible while avoiding too extreme and unsuitable values. We agreed not to analyze the infill pattern. According to the literature, the infill pattern mainly affects part mechanical properties, weight, and process time [40], but no significant impact on product quality is proven. Nevertheless, it is demonstrated that the gyroid infill pattern confers on the piece the best mechanical properties [40]. For this reason, we used this infill pattern for all our experiments. Finally, to avoid failure, such as completely detaching the piece from the heating plate, we covered the plate with a thin layer of solvent-free starch-based glue. Despite being very cheap and suitable for children's use, this glue worked very well, and it can be easily washed without the use of soaps or detergents.

3.5 Design of experiment

Since we have nine parameters on two levels, a full factorial Design of Experiment (DoE) would require 2^9 (512) tests. We, therefore, opted for an experimental plan with the Taguchi method formed by 32 orthogonal vectors (L32). Table 4 shows the entire experiment through 32 arrays based on the nine factors on two levels. The Taguchi method allows us to investigate the impact of different parameters with a small set of experiments. Moreover, this methodology is widely used in additive manufacturing scientific research [41]. In other applications, with higher budgets or fewer factors, the application of a full factorial is not to be ruled out.

3.6 Statistical analysis

Once all the experiments were performed, we studied the results in order to find the relations between the parameters and the measured performance. Since we have 11 qualitative indexes ($\overline{Q}_{ik}$), 3 resolution indexes ($\overline{R}_{ik}$), 11 accuracy indexes ($\overline{A}_{ik}$) and 4 Environmental-Related Performances (PE_i, w_i, PT_i, and $totC_i$) for each i-th part, we have to find 29 different functions. However, since the $totC_i$ equation is a combination of PE_i, w_i and constants, it was not necessary to estimate it by a regression. Therefore, we tried to develop 28 regression models to analyze the relations between the parameters and the performances. We decided to evaluate the qualitative, resolution, and accuracy models separately since these indexes represent different objectives. For instance, $\overline{Q}_{ik}$ and $\overline{A}_{ik}$ are correlated. However, these two metrics do not represent precisely the same thing; geometric analysis of the cloud of points can detect any deviation from the reference. On the other hand, the visual-qualitative assessment examines the surface quality, smoothness of structures

and overhangs, and the aesthetic of the parts, features not detectable through the scanner.

In order to find the best model to predict the impact of parameters on performances, we used a methodology composed of 3 different steps: (i) outliers analysis, (ii) stepwise bidirectional regression fitting minimizing the model AIC [42], (iii) and finally a backward elimination of the less significant predictors to avoid overfitting. In order to prevent multicollinearity, the three binomial variables (S, BAS, and RE) have been substituted with three binary variables (SY, BASY, and REY), indicating if supports are used, if a base is used and if the part is produced with recycled material. Finally, each model's normality and homoscedastic residuals have been tested using a Shapiro–Wilk test [43] and the studentized Breusch–Pagan test [44]. The models' reliability varies greatly depending on the sub-part being evaluated. We decided to place a 40% R2 threshold on the models. All models that explain less than 40% of the variance are not reported, so these features cannot be evaluated in our case study. We unsuccessfully build a satisfactory model for seven performances: Arc $\overline{Q}$, Pin $\overline{R}$, Side $\overline{A}$, Rib $\overline{Q}$, 60° $\overline{Q}$, 30° $\overline{Q}$, and 45° $\overline{Q}$. Although these models cannot be used to predict, they still have interest, as they can express which factors among those studied have an impact (albeit minimal) on performance. Lastly, we managed to compute 21 out of 28 regression models. Table 5 displays models' significance with the associated R^2 adjusted and the p-value. The models details are reported in the appendix of this paper.

Table 6 shows a summary of the presented analysis. In particular, it is represented the occurrence of each factor with more than a single occurrence with two different percentages indicating how many times an increase of the parameter has a beneficial or detrimental effect on the studied performances.

3.7 Optimization problem definition

In this paragraph, the optimization problem is defined. Equation 6 represents all 22 objectives to be minimized. As previously mentioned, all variables presented reach their optimum in the minimum value. Equations 7a–u are precisely the 21 empirical regression models obtained by the statistical analysis of the 21 performances presented in the previous chapter. Equation 7v represents the kg of CO_2eq emitted in the atmosphere to produce the parts. This equation is derived from the general one presented before. In particular, in this mathematical function, it is inserted the binary variable RE_y, equal to 1 if recycled PLA is used, 0 otherwise, and the parameters are specified: ke is the CO_2eq emitted to produce a kg/VAh (in this analysis, we approximate this value as 0.06 CO_2eq kg/kWh, considering equal the CO_2eq released to generate a kWh or a kVAh), EE_{NRE} is the embedded energy in non-recycled PLA (15.28 kWh/kg), while EE_{RE} is the embedded energy in recycled PLA (5 kWh/kg). C_{NRE}

Table 4 L32 Taguchi design of experiment

ID	M	WT	PT	WS	S	BAS	LH	IR	SN
E1	−	−	−	−	−	−	−	−	−
E2	−	−	−	−	+	−	+	+	+
E3	−	−	−	+	−	+	−	+	+
E4	−	−	−	+	+	+	+	−	−
E5	−	−	+	−	−	+	+	−	+
E6	−	−	+	−	+	+	−	+	−
E7	−	−	+	+	−	−	+	+	−
E8	−	−	+	+	+	−	−	−	+
E9	−	+	−	−	−	+	+	+	−
E10	−	+	−	−	+	+	−	−	+
E11	−	+	−	+	−	−	+	−	+
E12	−	+	−	+	+	−	−	+	−
E13	−	+	+	−	−	−	−	+	+
E14	−	+	+	−	+	−	+	−	−
E15	−	+	+	+	−	+	−	−	−
E16	−	+	+	+	+	+	+	+	+
E17	+	−	−	−	−	+	+	+	+
E18	+	−	−	−	+	+	−	−	−
E19	+	−	−	+	−	−	+	−	−
E20	+	−	−	+	+	−	−	+	+
E21	+	−	+	−	−	−	−	+	−
E22	+	−	+	−	+	−	+	−	+
E23	+	−	+	+	−	+	−	−	+
E24	+	−	+	+	+	+	+	+	−
E25	+	+	−	−	−	−	−	−	+
E26	+	+	−	−	+	−	+	+	−
E27	+	+	−	+	−	+	−	+	−
E28	+	+	−	+	+	+	+	−	+
E29	+	+	+	−	−	+	+	−	−
E30	+	+	+	−	+	+	−	+	+
E31	+	+	+	+	−	−	+	+	+
E32	+	+	+	+	+	−	−	−	−

is the CO_2eq released to produce 1 kg of non-recycled PLA (2.8 CO_2eq kg/kg) and C_{RE} for recycled one (0.95 CO_2eq kg/kg). Finally, Eqs. 8a–i represent the decisional variables' lower and upper bound. The range is the same as the experimental plan. Since we have studied only this space, we can infer only inside it.

$$\min PT, PE, w, totC, \overline{A}_B, \overline{Q}_B, \overline{A}_A, \overline{A}_{Sp}, \overline{Q}_{Sp},$$
$$\overline{A}_P, \overline{Q}_P, \overline{Q}_{Sd}, \overline{R}_{Sd},$$
$$\overline{A}_H, \overline{Q}_H, \overline{A}_{Sl}, \overline{Q}_{Sl}, \overline{A}_R, \overline{R}_R, \overline{A}_S, \overline{A}_F, \overline{A}_T \quad (6)$$

$$PT = k_{PT} - \hat{\beta}_{1PT} \cdot WS + \hat{\beta}_{2PT} \cdot S_y + \hat{\beta}_{3PT} \cdot BAS_y + \hat{\beta}_{4PT} \cdot LH$$
$$+ \hat{\beta}_{5PT} \cdot IR + \hat{\beta}_{6PT} \cdot SN + \hat{\beta}_{7PT} \cdot LH \cdot SN$$

$$+ \hat{\beta}_{8PT} \cdot LH \cdot IR + \hat{\beta}_{9PT} \cdot IR \cdot SN \quad (7a)$$

$$PE = k_{PE} + \hat{\beta}_{1PE} \cdot PT + \hat{\beta}_{2PE} \cdot WS + \hat{\beta}_{3PE} \cdot S_y + \hat{\beta}_{4PE} \cdot LH$$
$$+ \hat{\beta}_{5PE} \cdot IR - \hat{\beta}_{6PE} \cdot LH \cdot IR \quad (7b)$$

$$w = k_w + \hat{\beta}_{1w} \cdot S_y + \hat{\beta}_{2w} \cdot BAS_y + \hat{\beta}_{3w} \cdot LH + \hat{\beta}_{4w} \cdot IR + \hat{\beta}_{5w} \cdot SN \quad (7c)$$

$$\overline{A}_B = k_{\overline{A}_B} + \hat{\beta}_{1\overline{A}_B} \cdot S_y + \hat{\beta}_{2\overline{A}_B} \cdot LH + \hat{\beta}_{3\overline{A}_B} \cdot SN + \hat{\beta}_{4\overline{A}_B} \cdot S_y \cdot SN \quad (7d)$$

$$\overline{Q}_B = k_{\overline{Q}_B} + \hat{\beta}_{1\overline{Q}_B} \cdot RE_y + \hat{\beta}_{2\overline{Q}_B} \cdot WS + \hat{\beta}_{3\overline{Q}_B} \cdot S_y + \hat{\beta}_{4\overline{Q}_B} \cdot LH \quad (7e)$$

$$\overline{A}_A = k_{\overline{A}_A} + \hat{\beta}_{1\overline{A}_A} \cdot RE_y + \hat{\beta}_{2\overline{A}_A} \cdot WS + \hat{\beta}_{3\overline{A}_A} \cdot S_y + \hat{\beta}_{4\overline{A}_A} \cdot IR$$
$$+ \hat{\beta}_{5\overline{A}_A} \cdot BAS_y \cdot WS + \hat{\beta}_{6\overline{A}_A} \cdot BAS_y \cdot S_y + \hat{\beta}_{7\overline{A}_A} \cdot BAS_y \cdot RE_y \quad (7f)$$

Table 5 Regression models significance

Dep. variable	Adj-R^2 (%)	P-value
Bridge $\overline{A}_B$	78.85	1.45E−09
Bridge $\overline{Q}_B$	70.97	9.64E−08
Arc $\overline{A}_A$	58.69	1.01E−04
Sphere $\overline{A}_{Sp}$	62.51	2.36E−04
Sphere $\overline{Q}_{Sp}$	47.52	2.37E−04
Pin $\overline{A}_P$	59.40	1.20E−05
Pin $\overline{Q}_P$	44.28	1.95E−03
Side $\overline{Q}_{Sd}$	57.50	7.21E−05
Side $\overline{R}_{Sd}$	63.35	4.97E−07
Hole $\overline{A}_H$	45.97	2.51E−04
Hole $\overline{Q}_H$	46.75	7.69E−05
Slot $\overline{A}_{Sl}$	71.26	1.53E−07
Slot $\overline{Q}_{Sl}$	55.78	1.09E−05
Ribs $\overline{A}_R$	72.39	1.36E−08
Ribs $\overline{R}_R$	58.81	3.41E−06
60°$\overline{A}_S$	64.23	8.07E−07
45°$\overline{A}_F$	39.68	4.14E−04
30°$\overline{A}_T$	80.33	5.53E−10
PT	98.80	2.20E−16
PE	93.67	6.35E−15
w	95.35	2.20E−16

Table 6 Factors occurrences and their impacts

Factor	Occurrences	Beneficial effect (%)	Detrimental effect (%)
LH	14	64	36
WS	9	33	67
S$_Y$	8	63	38
SN	7	57	43
BAS$_Y$	5	40	60
IR	5	40	60
RE$_Y$	4	50	50
WT	4	0	100
LH × SN	4	50	50
PT	3	67	33
LH × WS	3	0	100
RE$_Y$ × LH	3	67	33
S$_Y$ × SN	2	50	50
BAS$_Y$ × LH	2	0	100
RE$_Y$ × WT	2	100	0
LH × PT	2	50	50
LH × IR	2	100	0

$$\overline{A}_{Sp} = k_{\overline{A}_{Sp}} + \hat{\beta}_{1\overline{A}_{Sp}} \cdot WT + \hat{\beta}_{2\overline{A}_{Sp}} \cdot PT + \hat{\beta}_{3\overline{A}_{Sp}} \cdot WS - \hat{\beta}_{4\overline{A}_{Sp}} \cdot S_y$$
$$+ \hat{\beta}_{5\overline{A}_{Sp}} \cdot LH + \hat{\beta}_{6\overline{A}_{Sp}} \cdot LH \cdot PT + \hat{\beta}_{7\overline{A}_{Sp}} \cdot LH \cdot S_y + \hat{\beta}_{8\overline{A}_{Sp}} \cdot PT \cdot S_y$$
$$(7g)$$

$$\overline{Q}_{Sp} = k_{\overline{Q}_{Sp}} + \hat{\beta}_{1\overline{Q}_{Sp}} \cdot WT + \hat{\beta}_{2\overline{Q}_{Sp}} \cdot SN + \hat{\beta}_{3\overline{Q}_{Sp}} \cdot LH \cdot WS \quad (7h)$$

$$\overline{A}_P = k_{\overline{A}_P} + \hat{\beta}_{1\overline{A}_P} \cdot PT + \hat{\beta}_{2\overline{A}_P} \cdot WS + \hat{\beta}_{3\overline{A}_P} \cdot LH + \hat{\beta}_{4\overline{A}_P} \cdot IR \quad (7i)$$

$$\overline{Q}_P = k_{\overline{Q}_P} + \hat{\beta}_{1\overline{Q}_P} \cdot RE_y + \hat{\beta}_{2\overline{Q}_P} \cdot WT + \hat{\beta}_{3\overline{Q}_P} \cdot WS$$
$$+ \hat{\beta}_{4\overline{Q}_P} \cdot SN + \hat{\beta}_{5\overline{Q}_P} \cdot RE_y \cdot WT + \hat{\beta}_{6\overline{Q}_P} \cdot LH \cdot PT$$
$$(7j)$$

$$\overline{Q}_{Sd} = k_{\overline{Q}_{Sd}} + \hat{\beta}_{1\overline{Q}_{Sd}} \cdot WS + \hat{\beta}_{2\overline{Q}_{Sd}} \cdot LH + \hat{\beta}_{3\overline{Q}_{Sd}} \cdot SN$$
$$+ \hat{\beta}_{4\overline{Q}_{Sd}} \cdot SN \cdot LH + \hat{\beta}_{5\overline{Q}_{Sd}} \cdot RE_y \cdot LH \quad (7k)$$

$$\overline{R}_{Sd} = k_{\overline{R}_{Sd}} + \hat{\beta}_{1\overline{R}_{Sd}} \cdot LH + \hat{\beta}_{2\overline{R}_{Sd}} \cdot LH \cdot WS \quad (7l)$$

$$\overline{A}_H = k_{\overline{A}_H} + \hat{\beta}_{1\overline{A}_H} \cdot WS + \hat{\beta}_{2\overline{A}_H} \cdot LH \cdot WT + \hat{\beta}_{3\overline{A}_H} \cdot WS \cdot WT$$
$$(7m)$$

$$\overline{Q}_H = k_{\overline{Q}_H} + \hat{\beta}_{1\overline{Q}_H} \cdot LH + \hat{\beta}_{2\overline{Q}_H} \cdot SN \quad (7n)$$

$$\overline{A}_{Sl} = k_{\overline{A}_{Sl}} + \hat{\beta}_{1\overline{A}_{Sl}} \cdot LH + \hat{\beta}_{1\overline{A}_{Sl}} \cdot LH \cdot SN$$
$$+ \hat{\beta}_{1\overline{A}_{Sl}} \cdot RE_y \cdot SN + \hat{\beta}_{1\overline{A}_{Sl}} \cdot RE_y \cdot LH \quad (7o)$$

$$\overline{Q}_{Sl} = k_{\overline{Q}_{Sl}} + \hat{\beta}_{1\overline{Q}_{Sl}} \cdot BAS_y + \hat{\beta}_{2\overline{Q}_{Sl}} \cdot LH \quad (7p)$$

$$\overline{A}_R = k_{\overline{A}_R} + \hat{\beta}_{1\overline{A}_R} \cdot BAS_y + \hat{\beta}_{2\overline{A}_R} \cdot LH + \hat{\beta}_{3\overline{A}_R} \cdot BAS_y \cdot LH$$
$$(7q)$$

$$\overline{R}_R = k_{\overline{R}_R} + \hat{\beta}_{1\overline{R}_R} \cdot LH \cdot BAS_y + \hat{\beta}_{2\overline{R}_R}$$
$$\cdot LH \cdot WS + \hat{\beta}_{3\overline{R}_R} \cdot RE_y \cdot LH \quad (7r)$$

$$\overline{A}_S = k_{\overline{A}_S} + \hat{\beta}_{1\overline{A}_S} \cdot RE_y + \hat{\beta}_{2\overline{A}_S} \cdot WT + \hat{\beta}_{2\overline{A}_S} \cdot RE_y \cdot WT$$
$$(7s)$$

$$\overline{A}_F = k_{\overline{A}_F} + \hat{\beta}_{1\overline{A}_F} \cdot S_y + \hat{\beta}_{2\overline{A}_F} \cdot PT \cdot SN \quad (7t)$$

$$\overline{A}_T = k_{\overline{A}_T} + \hat{\beta}_{1\overline{A}_T} \cdot BAS_y + \hat{\beta}_{2\overline{A}_T} \cdot LH$$
$$+ \hat{\beta}_{3\overline{A}_T} \cdot S_y \cdot SN + \hat{\beta}_{4\overline{A}_T} \cdot SN \cdot LH \quad (7u)$$

$$totC = ke \cdot EE_{RE} \cdot w \cdot RE_y + C_{RE} \cdot w \cdot RE_y$$
$$+ ke \cdot EE_{NRE} \cdot w \cdot (1 - RE_y)$$
$$+ C_{NRE} \cdot w \cdot (1 - RE_y) + ke \cdot PE \quad (7v)$$

$$s.t.$$

$$\{RE_y \in \mathbb{N} | 0 \leq RE_y \leq 1\} \quad (8a)$$

$$\{WT \in \mathbb{R} | 200 \leq WT \leq 215\} \tag{8b}$$

$$\{PT \in \mathbb{R} | 25 \leq PT \leq 50\} \tag{8c}$$

$$\{WS \in \mathbb{R} | 40 \leq WS \leq 80\} \tag{8d}$$

$$\{BAS_y \in \mathbb{N} | 0 \leq BAS_y \leq 1\} \tag{8e}$$

$$\{S_y \in \mathbb{N} | 0 \leq S_y \leq 1\} \tag{8f}$$

$$\{LH \in \mathbb{R} | 0.1 \leq LH \leq 0.3\} \tag{8g}$$

$$\{IR \in \mathbb{R} | 10 \leq IR \leq 60\} \tag{8h}$$

$$\{SN \in \mathbb{N} | 1 \leq SN \leq 3\} \tag{8i}$$

In order to find the best solution, we implemented the problem in Python using the pymoo library [45]. In particular, we used the NSGA-II algorithm [46]. In the literature, it is possible to find some recent applications of NSGA-II on additive manufacturing optimization. E.g., in [47], the authors used the same algorithm to find a frontier of solutions that minimize the time and material consumption while keeping a sufficient level of ultimate tensile strength and surface roughness. Matos et al. [48] studied the best manufacturing positioning while optimizing the support area, the manufacturing time, the surface roughness and the surface quality using an NSGA-II algorithm.

The algorithm NSGA-II generates an initial population P_t of solutions with dimension N. Then a mutation operation is performed to create an offspring O_t of size N. The two populations, P_t and O_t, are combined to form Z_t. Then the solutions are sorted according to non-domination criteria; each solution front is ranked according to this criterion. The following population P_{t+1} is generated, taking the first-ranked front. If the first front is less than N, other solutions are taken from the least crowded region of the second front, and this procedure continues by the lower-ranked fronts until a P_{t+1} population of size N is obtained [46].

The new offspring O_t, depends on two operators: the crossover probability X and the mutation probability M. Finally, to find the best solutions, four different factors have to be set: the population (N), the crossover (X) and the mutation (M) and the number of generations to be tested (G). In the literature, it is possible to find different suggestions and methods for choosing these parameters. According to Schaffer et Al. [49], a mutation probability higher than 0.05 never drives good results, and M of 0.005 and a X between 0.95 and 0.65, even with a small population, is suggested. For these reasons, we decided to set a $M = 0.005$ and a X equal to

0.95. Finally in order to increase the probability to reach te convergence we set a number of generation G equal to 1000.

According to the literature, the larger the initial population, the more efficiently the algorithm finds the optimal front [50]. For this reason, we tested the difference between the optimal frontier obtained with a N equal to 1000, 35, 30 and 20. The difference between the first ($N = 1000$) and the second ($N = 35$) is meagre: looking for the best solution in each performance, these were practical all the same, and only one deviated by less than 2%. While testing the first with the third, all values were identical except for one value that differed by about 10%. Finally, as expected, we got the worst results with a population of only 20 solutions. The average deviation from the first run was 20%, with peaks at 117%. For this reason, we can assume that the best value for N would be between 30 and 35. So, for this reason, we fixed N equal to 35, testing 35,000 solutions. The results have been obtained with a computer HP Elitebook 830 G6 with CPU Intel core i5-8265U 1.60 GHz and RAM 16 GB. The algorithm evaluates 1000 generations made of a population of 1000 in about 9 min and 2 s. In contrast, it tests 1000 generations of 35 solutions on average in 37 s.

3.8 Multi-criteria decision method

Once the result is obtained, the second problem is determining the best solution. For this reason, we proposed a methodology to use this solution and help the designer decide. We proposed a visual method in order to facilitate decision-making.

The heatmap presented in Fig. 7 represents the 35 different solutions obtained through the optimization algorithm. On the x-axis are present the 22 performances, while the y-axis shows the solution ID between 1 to 35. In each square, the value of the performance is represented using a color scale from red to green. The best performance is represented with green color, while the worst one is in red. This chart can be used as a map for the designer to choose the best parameters and can be made available near the workstation or machine.

For instance, if the designer has to produce a part with a bridge in the lesser time possible. A possible approach could be to see the dark green square corresponding to the non-dominated solutions in the T column. Solution 27 (light blue) seems to be the faster one. Nevertheless, analyzing the Ab and Qb columns, we immediately see that the corresponding quality of the bridge is low. Solution 18 (navy blue) is sufficiently fast and has a satisfactory accuracy index. Finally, after thoroughly analyzing the results, it is possible to find solution 19 (magenta), which seems to be an average process time and a good bridge quality as a whole. The three proposed solutions are graphically depicted in Figs. 8 and 9 The former represents the status of the nine parameters in each solution, and the latter shows the value of the 22 performances. The

Fig. 7 Solution Heatmap with solutions 18, 19 and 27 highlighted (the last three variables, T, E, M and C, stand for process time, energy consumption, material consumption, and CO_2eq)
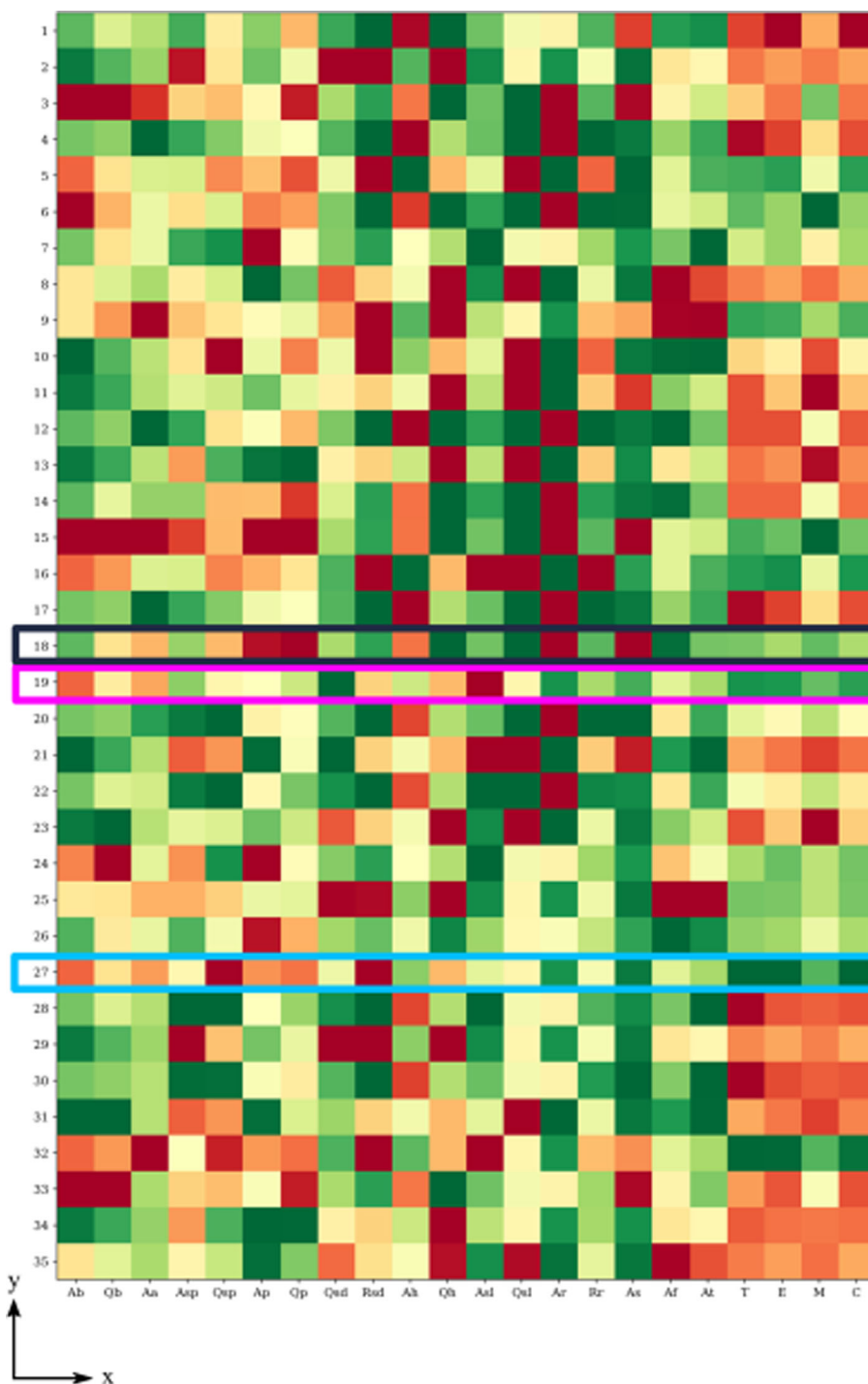
three solutions are presented as a single-colored line (navy blue for solution 18, magenta for 19, and light blue for 27, they are also highlighted in Fig. 7 the same colors). The y-axis of the two images is normalized to represent the top and bottom levels efficiently. While Fig. 9 the y-axis is also inverted since the objective is to minimize the 22 performances, this representation can be straightforwardly understood, and the better value is on top of the graph.

As can be seen from Fig. 9, the three solutions differ significantly from each other. None of the three needs a base, those with better arcs require support and have a lower layer height. In comparison, the fastest one has all the parameters set to finish as fast as possible: no base or support, only one shell number, high working speed, high layer height, and an infill rate of 10%.
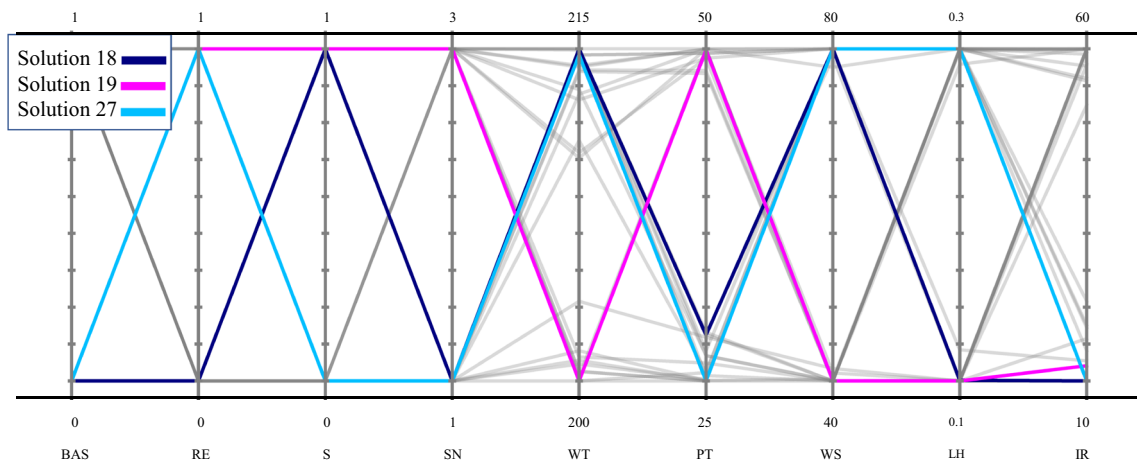
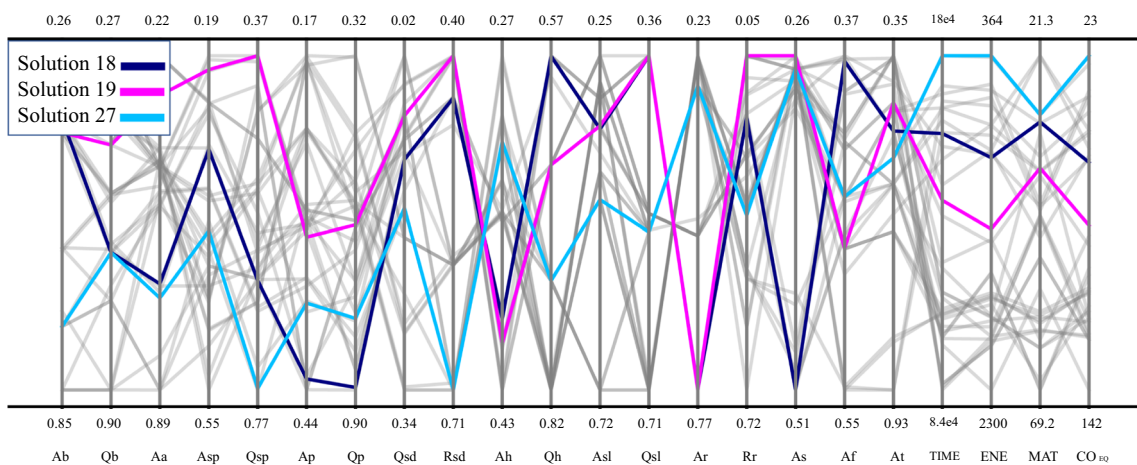**Fig. 8** Parameter selection of solutions 18, 19 and 27

Fig. 9 Performance Representation of solutions 18, 19, and 27

The designer should be able to decide which solution is most suitable for him, looking at Fig. 7. The fastest one (27) should be enough if it is just a tester or a prototype. If he is not interested in the externally perceived quality, solution 18 can guarantee good accuracy in a short time. While if a good arc is needed, the best solution is the 19.

4 Discussion and future developments

Additive manufacturing offers numerous advantages over traditional manufacturing processes, such as producing low-volume, customized products with complex geometries and advanced material properties. However, one of the challenges additive manufacturing faces is the lack of repeatability in the final product, which can result in variations in shape, dimensional accuracy, and mechanical properties. The outcome of the manufacturing process can vary significantly in shape, dimensional accuracy, and mechanical properties, leading to inconsistencies in the final product [51]. Overcoming these challenges is crucial for the widespread adoption and realization of the full potential of additive manufacturing. For

this reason, the present study aims to propose a methodology suitable to help designers in preconizing the results of the production. In this way, waste can be limited. This issue can be even more pronounced in one-of-a-kind productions, where the users do not have much experience with the product they are designing and the risk of causing waste is even more evident. The paper proposes a methodology for generating knowledge in OKP additive manufacturing contexts. In such a context, testing and manufacturing various parts to evaluate the best set of production parameters is not allowed. Therefore, the designer needs decision support tools.

The method presented aims to study the product both in terms of production cost (seen as consumption of energy, time, and matter) and environmental impact (evaluated by a semi-quantitative method that can estimate the CO_2eq emitted) and quality, assessed through three metrics representing accuracy, resolution, and subjective perceived quality. In this way the user is involved in this choice and therefore he will be more conscious and lead to less waste. Involving end-users and other stakeholders in the early design stages of additive

manufacturing can bring several potential benefits. Any necessary changes or improvements can be made early on, saving time and resources in the long run. Additionally, involving stakeholders and end-users at this early stage can create a sense of commitment and ownership towards the technology being developed, leading to increased engagement and support throughout the rest of the development process and awareness of intellectual proprietary rights. This can result in the creation of innovative solutions and the avoidance of design and construction waste. Furthermore, early involvement allows for a better understanding of end-user processes, leading to improved construction productivity and the ability to design constructs or services that are tailored to their specific requirements.

The proposed methodology aims to model the impacts of parameters on the described performance through a statistical-empirical analysis. The regression models are finally used to find a set of Pareto non-dominated solutions. Ultimately, these solutions are implemented in a visualization-based decision-making support procedure. The results obtained are quite satisfactory, and many prediction models succeed in describing a large part of the variability of the process. We obtained 21 out of 28 models that describe at least 45% of the variability. In addition, the models related to energy consumption, material consumption, and production time represented the process very well by describing more than 90% of the variability. As expected, the prediction of geometric accuracy output is very difficult especially in some cases involving curvilinear parts (Arcs, Spheres, Holes, and Pins), while we get very good results in larger and less complex parts such as Bridges and Slopes. More analysis will need to be done in the future to make the results predictable and repeatable to avoid waste.

Finally, the application of the proposed method leads to the creation of an easily readable visual-based poster that can guide the user in OKP or DIY contexts in choosing production parameters. This type of poster can find easy application in FabLabs or small laboratories, moreover 3D printer manufacturers could propose such a tool to guide their users in facilitating the use of the machine.

The main limitation of the present work is the lack of validation of the method through the design of a real part. This validation can undoubtedly be a future work assuming that the heatmap presented can be used to support the design work of a new product.

A second limitation of the work is its lack of joints, threaded parts, and other complex features in the studied benchmark. It only focuses on analyzing basic geometric shapes, which limits its ability to evaluate the capabilities of additive manufacturing systems in fabricating functional parts with intricate designs. The absence of joints and threaded parts in the benchmark restricts the assessment of the assembly and connectivity aspects of additively manufactured components. Furthermore, the benchmark does not include an analysis of the mechanical properties of the printed parts. Mechanical performance is a crucial factor in determining the functionality and reliability of AM components. To address these limitations, future work should consider improving the benchmark to include joints, threaded parts, and other complex features commonly found in functional components. This expansion would enable a more realistic assessment of the additive manufacturing systems' capabilities in producing parts that require assembly and have intricate geometries. Additionally, incorporating an analysis of the mechanical properties of the fabricated parts would provide valuable insights into their structural integrity, strength, and durability.

Finally, According to [21], a simple regression model combined with physic/equation-based modeling can outperform machine learning approaches in small dataset applications. Generating large datasets to test manufacturing could often prove inconvenient, particularly in OKP productions. Combining the proposed experimental approach with physic-based models can be interesting as a future improvement.

Data availability Data supporting the findings of this study (CAD file, mesh file, scanning stl files, the cloud of points files, time series of energy consumption of the 32 tests, and the dataset of material consumption and processing time) are available from the corresponding author on request.

Code availability The code of the regression and optimization models is available from the corresponding author on request.

Declarations

Appendix

See Tables 7, 8, 9, 10, 11, 12, 13, 14, 15 and 16.

Table 7 Bridge models

Dep. variable	Predictors	β	Sig	Adj-R^2	p-value
Bridge $\overline{A}_B$	Constant	0.97379	***	78.85%	1.45E−09
	S_Y	− 0.56082	***		
	LH	− 0.56170	**		
	SN	− 0.06975	*		
	$S_Y \times SN$	0.08170	*		
Bridge $\overline{Q}_B$	Constant	0.75909	***	70.97%	9.64E−08
	RE_Y	− 0.09091	*		
	WS	0.00278	**		
	S_Y	− 0.25909	***		
	LH	− 0.84091	***		

*** < 0.1%, ** < 1%, * < 5%, and † < 10%

Table 8 Arc model

Dep. variable	Predictors	β	Sig	Adj-R^2	p-value
Arc $\overline{A}_A$	Constant	0.52291	***	58.69%	1.01E−04
	RE_Y	− 0.18445	**		
	WS	0.00473	***		
	S_Y	− 0.21279	***		
	IR	− 0.00166	*		
	$BAS_Y \times WS$	− 0.00476	***		
	$BAS_Y \times S_Y$	0.22654	**		
	$BAS_Y \times RE_Y$	0.18686	*		

*** < 0.1%, ** < 1%, * < 5%, and † < 10%

Table 9 Sphere models

Dep. variable	Predictors	β	Sig	Adj-R^2	P-value
Sphere $\overline{A}_{Sp}$	Constant	− 0.07086		62.51%	2.36E−04
	WT	0.00324	†		
	PT	− 0.00652	*		
	WS	0.00127	*		
	S_Y	− 0.42845	***		
	LH	− 1.37713	**		
	$LH \times PT$	0.03026	**		
	$LH \times S_Y$	1.10383	***		
	$PT \times S_Y$	0.00410	*		
Sphere $\overline{Q}_{Sp}$	Constant	− 0.77312		47.52%	2.37E−04
	WT	0.00657	*		
	SN	− 0.06777	**		
	$LH \times WS$	0.00816	**		

*** < 0.1%, ** < 1%, * < 5%, and † < 10%

Table 10 Pins models

Dep. variable	Predictors	β	Sig	Adj-R^2	P-value
Pin $\overline{A}_P$	Constant	0.43845	***	59.40%	1.20E−05
	PT	− 0.00251	**		
	WS	0.00140	**		
	LH	− 0.34794	**		
	IR	− 0.00157	***		
Pin $\overline{Q}_P$	Constant	− 1.96121		44.28%	1.95E−03
	RE_Y	3.13450			
	WT	0.01250	*		
	WS	0.00326	*		
	SN	− 0.05028	*		
	$RE_Y \times$ WT	− 0.01486	*		
	LH $\times$ PT	− 0.01320	*		

*** $< 0.1\%$, ** $< 1\%$, * $< 5\%$, and † $< 10\%$

Table 11 Side models

Dep. variable	Predictors	β	Sig	Adj-R^2	p-value
Side $\overline{Q}_{Sd}$	Constant	0.09507		57.50%	7.21E−05
	WS	0.00131	*		
	LH	− 0.69415	*		
	SN	− 0.05635	*		
	LH $\times$ SN	0.47083	***		
	$RE_Y \times$ LH	0.29911	*		
Side $\overline{R}_{Sd}$	Constant	0.30483	***	63.35%	4.97E−07
	LH	0.57648	*		
	LH $\times$ WS	0.00954	*		

*** $< 0.1\%$, ** $< 1\%$, * $< 5\%$, and † $< 10\%$

Table 12 Holes models

Dep. variable	Predictors	β	Sig	Adj-R^2	p-value
Hole $\overline{A}_H$	Constant	0.50310	***	45.97%	2.51E−04
	WS	− 0.01003	*		
	LH $\times$ WT	− 0.00197	***		
	WS $\times$ WT	0.00004	*		
Hole $\overline{Q}_H$	Constant	0.43806	***	46.75%	7.69E−05
	LH	0.85751	***		
	SN	0.04167	*		

*** $< 0.1\%$, ** $< 1\%$, * $< 5\%$, and † $< 10\%$

Table 13 Slot models

Dep. variable	Predictors	β	Sig	Adj-R^2	p-value
Slot $\overline{A}_{Sl}$	Constant	0.16499	***	71.26%	1.53E−07
	LH	2.38415	***		
	LH × SN	− 0.51907	***		
	RE$_Y$ × SN	0.07145	**		
	RE$_Y$ × LH	− 1.14278	***		
Slot $\overline{Q}_{Sl}$	Constant	0.27139	***	55.78%	1.09E−05
	BAS$_Y$	0.16479	***		
	LH	0.92009	***		

*** < 0.1%, ** < 1%, * < 5%, and † < 10%

Table 14 Ribs models

Dep. variable	Predictors	β	Sig	Adj-R^2	p-value
Ribs $\overline{A}_R$	Constant	1.01471	***	72.39%	1.36E−08
	BAS$_Y$	− 0.34764	**		
	LH	− 2.44407	***		
	BAS$_Y$ × LH	0.99662	*		
Ribs $\overline{R}_R$	Constant	0.01307		58.81%	3.41E−06
	BAS$_Y$ × LH	0.74182	**		
	LH × WS	0.02013	***		
	RE$_Y$ × LH	− 0.41887	†		

*** < 0.1%, ** < 1%, * < 5%, and † < 10%

Table 15 Slope models

Dep. variable	Predictors	β	Sig	Adj-R^2	p-value
60°$\overline{A}_S$	Constant	− 2.82137	***	64.23%	8.07E−07
	RE$_Y$	2.94402	***		
	WT	0.01549	***		
	RE$_Y$ × WT	− 0.01481	***		
45°$\overline{A}_F$	Constant	0.42493	***	39.68%	4.14E−04
	S$_Y$	− 0.07680	**		
	PT × SN	0.00084	**		
30°$\overline{A}_T$	Constant	0.59589	***	80.33%	5.53E−10
	BAS$_Y$	− 0.08056	**		
	LH	− 0.88281	***		
	S$_Y$ × SN	− 0.09045	***		
	LH × SN	0.66164	***		

*** < 0.1%, ** < 1%, * < 5%, and † < 10%

Table 16 Environmental-related performances models

Dep. variable	Predictors	β	Sig	Ad-R^2	p-value
PT	Constant	26,559.33	***	98.80%	2.20E−16
	WS	− 62.36	***		
	S$_Y$	5016.69	***		
	BAS$_Y$	1196.56	***		
	LH	− 51,749.37	***		
	IR	757.3	***		
	SN	4458.51	***		
	LH × SN	− 7974.69	*		
	LH × IR	− 1785.44	***		
	IR × SN	− 53.15	*		
PE	Constant	697.213	***	93.67%	6.35E−15
	PT	11.978	***		
	WS	− 2.802	*		
	S$_Y$	149.375	**		
	LH	− 2012.881	***		
	IR	19.546	***		
	LH × IR	− 54.093	***		
w	Constant	11.34462	***	95.35%	2.20E−16
	S$_Y$	9.5	***		
	BAS$_Y$	10.55	***		
	LH	42.45	***		
	IR	0.26823	***		
	SN	3.01313	***		

*** $< 0.1\%$, ** $< 1\%$, * $< 5\%$, and † $< 10\%$

References

1. Koren, Y., Gu, X., Guo, W.: Reconfigurable manufacturing systems: principles, design, and future trends. Front. Mech. Eng. **13**, 121–136 (2018). https://doi.org/10.1007/s11465-018-0483-0

2. Gong, X., Jiao, R., Jariwala, A., Morkos, B.: Crowdsourced manufacturing cyber platform and intelligent cognitive assistants for delivery of manufacturing as a service: fundamental issues and outlook. Int. J. Adv. Manuf. Technol. **117**, 1997–2007 (2021). https://doi.org/10.1007/s00170-021-07789-7

3. Fisher, O., Watson, N., Porcu, L., et al.: Cloud manufacturing as a sustainable process manufacturing route. J. Manuf. Syst. **47**, 53–68 (2018). https://doi.org/10.1016/j.jmsy.2018.03.005

4. Barni, A., Carpanzano, E., Landolfi, G., Pedrazzoli, P.: Urban manufacturing of sustainable customer-oriented products. In: Monostori, L., Majstorovic, V.D., Hu, S.J., Djurdjanovic, D. (eds.) Proceedings of the 4th International Conference on the Industry 4.0 Model for Advanced Manufacturing, pp. 128–141. Springer International Publishing, Cham (2019)

5. Lanz, M., Järvenpää, E.: Social manufacturing and open design. Responsible Consum. Prod., 668–678 (2020)

6. Panza, L., Faveto, A., Bruno, G., Lombardi, F.: Open product development to support circular economy through a material lifecycle management framework. Int. J. Prod. Lifecycle Manag. (2022). https://doi.org/10.1504/IJPLM.2022.125826

7. Castiblanco Jimenez, I.A., Mauro, S., Napoli, D., et al.: Design thinking as a framework for the design of a sustainable waste sterilization system: the case of Piedmont region, Italy. Electronics **10**, 2665 (2021). https://doi.org/10.3390/electronics10212665

8. Mesa, D., Renda, G., Iii, R.G., et al.: Implementing a design thinking approach to de-risk the digitalisation of manufacturing SMEs. Sustainability **14**, 14358 (2022). https://doi.org/10.3390/su142114358

9. Tang, P., Sun, X., Law, E.L.-C., et al.: User-centered design approaches to integrating intellectual property information into early design processes with a design patent retrieval application. Int. J. Hum.-Comput. Interact. **36**, 911–929 (2020). https://doi.org/10.1080/10447318.2019.1699747

10. Pereira, T., Kennedy, J.V., Potgieter, J.: A comparison of traditional manufacturing vs additive manufacturing, the best method for the job. Procedia Manuf. **30**, 11–18 (2019). https://doi.org/10.1016/j.promfg.2019.02.003

11. Bruno, G., Faveto, A., Traini, E.: An open source framework for the storage and reuse of industrial knowledge through the integration of PLM and MES. Manag. Prod. Eng. Rev. **11**, 62–73 (2020)

12. d'Antonio, G., Segonds, F., Laverne, F., et al.: A framework for manufacturing execution system deployment in an advanced additive manufacturing process. Int. J. Prod. Lifecycle Manag. **10**, 1–19 (2017). https://doi.org/10.1504/IJPLM.2017.082996

13. Bikas, H., Lianos, A.K., Stavropoulos, P.: A design framework for additive manufacturing. Int. J. Adv. Manuf. Technol. **103**, 3769–3783 (2019). https://doi.org/10.1007/s00170-019-03627-z

14. Sini, F., Bruno, G., Chiabert, P., Segonds, F.: A lean quality control approach for additive manufacturing. In: Nyffenegger, F., Ríos, J., Rivest, L., Bouras, A. (eds.) Product Lifecycle Management Enabling Smart X, pp. 59–69. Springer International Publishing, Cham (2020)

15. Bocken, N., Ritala, P.: Six ways to build circular business models. J. Bus. Strategy (2021). https://doi.org/10.1108/JBS-11-2020-0258

16. Chong, S., Pan, G.-T., Khalid, M., et al.: Physical characterization and pre-assessment of recycled high-density polyethylene as 3D printing material. J. Polym. Environ. 25, 136–145 (2017). https://doi.org/10.1007/s10924-016-0793-4

17. Vidakis, N., Petousis, M., Maniadi, A., et al.: Sustainable additive manufacturing: mechanical response of acrylonitrile-butadiene-styrene over multiple recycling processes. Sustainability 12, 3568 (2020). https://doi.org/10.3390/su12093568

18. Singh, S., Singh, G., Prakash, C., Ramakrishna, S.: Current status and future directions of fused filament fabrication. J. Manuf. Process. 55, 288–306 (2020). https://doi.org/10.1016/j.jmapro.2020.04.049

19. Ngo, T.D., Kashani, A., Imbalzano, G., et al.: Additive manufacturing (3D printing): a review of materials, methods, applications and challenges. Compos. B Eng. 143, 172–196 (2018). https://doi.org/10.1016/j.compositesb.2018.02.012

20. Alizadeh, M., Esfahani, M.N., Tian, W., Ma, J.: Data-driven energy efficiency and part geometric accuracy modeling and optimization of green fused filament fabrication processes. J. Mech. Des. 142, 041701 (2020). https://doi.org/10.1115/1.4044596

21. Rai, R., Sahu, C.K.: Driven by data or derived through physics? A review of hybrid physics guided machine learning techniques with cyber-physical system (CPS) focus. IEEE Access 8, 71050–71073 (2020). https://doi.org/10.1109/ACCESS.2020.2987324

22. de Pastre, M.-A., Toguem Tagne, S.-C., Anwer, N.: Test artefacts for additive manufacturing: a design methodology review. CIRP J. Manuf. Sci. Technol. 31, 14–24 (2020). https://doi.org/10.1016/j.cirpj.2020.09.008

23. ISO 52902: 2019 - Additive manufacturing—Test artifacts—Geometric capability assessment of additive manufacturing systems. BSI (2019)

24. Binali, R., Kuntoğlu, M., Pimenov, D.Y., et al.: Advance monitoring of hole machining operations via intelligent measurement systems: a critical review and future trends. Measurement 201, 111757 (2022). https://doi.org/10.1016/j.measurement.2022.111757

25. Bousnina, K., Hamza, A., Yahia, N.B.: Energy optimization for milling 304L steel using artificial intelligence methods. Int. J. Automot. Mech. Eng. 19, 9928–9938 (2022). https://doi.org/10.15282/ijame.19.3.2022.05.0765

26. Hamza, A., Bousnina, K., Yahia, N.B.: An approach to the influence of the machining process on power consumption and surface quality during the milling of 304L austenitic stainless steel. J. Mech. Eng. Sci. 16, 9093–9109 (2022). https://doi.org/10.15282/jmes.16.3.2022.11.0720

27. Markou, F., Segonds, F., Rio, M., Perry, N.: A methodological proposal to link design with additive manufacturing to environmental considerations in the early design stages. Int. J. Interact. Des. Manuf. 11, 799–812 (2017). https://doi.org/10.1007/s12008-017-0412-1

28. Laverne, F., Bottacini, E., Segonds, F., et al.: TEAM: a tool for eco additive manufacturing to optimize environmental impact in early design stages. In: Chiabert, P., Bouras, A., Noël, F., Ríos, J. (eds.) Product Lifecycle Management to Support Industry 4.0, pp. 736–746. Springer International Publishing, Cham (2018)

29. Rocheton, B., Segonds, F., Laverne, F., Perry, N.: HESAM: a human centered sustainable additive manufacturing tool for early design stages. Comput.-Aided Des. Appl. 18, 258–271 (2020). https://doi.org/10.14733/cadaps.2021.258-271

30. Agrawal, R.: Sustainable design guidelines for additive manufacturing applications. Rapid Prototyp. J. 28, 1221–1240 (2022). https://doi.org/10.1108/RPJ-09-2021-0251

31. Kumar, K., Singh, V., Katyal, P., Sharma, N.: EDM μ-drilling in Ti-6Al-7Nb: experimental investigation and optimization using NSGA-II. Int. J. Adv. Manuf. Technol. 104, 2727–2738 (2019). https://doi.org/10.1007/s00170-019-04012-6

32. Feng, Q., Liu, L., Zhou, X.: Automated multi-objective optimization for thin-walled plastic products using Taguchi, ANOVA, and hybrid ANN-MOGA. Int. J. Adv. Manuf. Technol. 106, 559–575 (2020). https://doi.org/10.1007/s00170-019-04488-2

33. Mavris, D., DeLaurentis, D., Bandte, O., Hale, M.: A stochastic approach to multi-disciplinary aircraft analysis and design. In: 36th AIAA Aerospace Sciences Meeting and Exhibit. American Institute of Aeronautics and Astronautics, Reno, NV, U.S.A. (1998)

34. Ashby, M.F.: Chapter 6—Eco-data: values, sources, precision. In: Ashby, M.F. (ed.) Materials and the Environment, 3rd edn., pp. 107–147. Butterworth-Heinemann, Oxford (2021)

35. Ashby, M.F.: Appendix B—Eco- and supply-chain data. In: Ashby, M.F. (ed.) Materials and the Environment, 3rd edn., pp. 403–429. Butterworth-Heinemann, Oxford (2021)

36. Yu, L., Pan, Y., Wu, Y.: Research on data normalization methods in multi-attribute evaluation. In: 2009 International Conference on Computational Intelligence and Software Engineering, pp. 1–5. IEEE, Wuhan (2009)

37. Tootooni, M.S., Dsouza, A., Donovan, R., et al.: Assessing the geometric integrity of additive manufactured parts from point cloud data using spectral graph theoretic sparse representation-based classification. American Society of Mechanical Engineers Digital Collection (2017)

38. Lin, W.: Online quality monitoring in material extrusion additive manufacturing processes based on laser scanning technology. Precis. Eng. 60, 76–84 (2019)

39. Redwood, B., Schöffer, F., Garret, B.: The 3D printing handbook: technologies, design and applications. 3D Hubs (2017)

40. Pazhamannil, R.V., JishnuNamboodiri, V.N., Govindan, P., Edacherian, A.: Property enhancement approaches of fused filament fabrication technology: a review. Polym. Eng. Sci. (2022). https://doi.org/10.1002/pen.25948

41. Liu, X., Zhang, M., Li, S., et al.: Mechanical property parametric appraisal of fused deposition modeling parts based on the gray Taguchi method. Int. J. Adv. Manuf. Technol. 89, 2387–2397 (2017). https://doi.org/10.1007/s00170-016-9263-3

42. McCullagh, P., Nelder, J.A.: Generalized linear models. Routledge, Milton Park (2019)

43. Royston, P.: Remark AS R94: a remark on algorithm AS 181: the W-test for Normality. J. R. Stat. Soc.: Ser. C (Appl. Stat.) 44, 547–551 (1995). https://doi.org/10.2307/2986146

44. Breusch, T.S., Pagan, A.R.: A simple test for heteroscedasticity and random coefficient variation. Econometrica 47, 1287–1294 (1979). https://doi.org/10.2307/1911963

45. Blank, J., Deb, K.: Pymoo: multi-objective optimization in python. IEEE Access 8, 89497–89509 (2020). https://doi.org/10.1109/ACCESS.2020.2990567

46. Deb, K., Pratap, A., Agarwal, S., Meyarivan, T.: A fast and elitist multiobjective genetic algorithm: NSGA-II. IEEE Trans. Evol. Comput. 6, 182–197 (2002). https://doi.org/10.1109/4235.996017

47. Asadollahi-Yazdi, E., Gardan, J., Lafon, P.: Multi-objective optimization of additive manufacturing process. IFAC-PapersOnLine 51, 152–157 (2018). https://doi.org/10.1016/j.ifacol.2018.08.250

48. Matos, M.A., Rocha, A.M.A.C., Costa, L.A.: Many-objective optimization of build part orientation in additive manufacturing. Int. J. Adv. Manuf. Technol. 112, 747–762 (2021). https://doi.org/10.1007/s00170-020-06369-5

49. Schaffer, J.D., Caruana, R., Eshelman, L.J., Das, R.: A study of control parameters affecting online performance of genetic algorithms

for function optimization. In: Proceedings of the 3rd International Conference on Genetic Algorithms, pp. 51–60. Morgan Kaufmann Publishers Inc., San Francisco, CA, USA (1989)

50. Muhlenbein, H., Schlierkamp-Voosen, D.: Optimal interaction of mutation and crossover in the breeder genetic algorithm. In: Proceedings of the 5th International Conference on Genetic Algorithms, vol. 10, p. 648 (1983)

51. Borgue, O., Stavridis, J., Vannucci, T., et al.: Model-based design of am components to enable decentralized digital manufacturing systems. Proc. Des. Soc. **1**, 2127–2136 (2021). https://doi.org/10.1017/pds.2021.474